Available online at www.sciencedirect.com

ScienceDirect

www.elsevier.com/locate/jes

JES JOURNAL OF ENVIRONMENTAL SCIENCES

www.jesc.ac.cn

Probing and understanding interaction of Eu(III) with γ- alumina in presenceof malonic acid

Madhuri A Patel[1], *Aishwarya Soumitra Kar*[1,*], *Vaibhavi V Raut*[1], *B.S. Tomar*[2]

[1] *Radioanalytical Chemistry Division, Bhabha Atomic Research Centre, Mumbai 400085, India*
[2] *Homi Bhabha National Institute, Anushaktinagar, Mumbai 400094, India*

ARTICLE INFO

Article history:
Received 23 April 2020
Revised 17 July 2020
Accepted 18 July 2020
Available online 28 July 2020

Keywords:
Malonic acid
Eu(III)
γ-alumina
Sorption
ATR-FTIR
TRFS
Surface complexation modeling

ABSTRACT

Radionuclide migration in aquatic environment is influenced by its sorption onto colloids/mineral oxides and the presence of organic complexing anions. With a view to understand the sorption of trivalent actinides by mineral oxides in presence of organic acid, in the present study, Eu(III), malonic acid (MA) and γ-alumina are considered as representatives of trivalent actinides, low molecular weight natural occurring organic acid and aluminol sites, respectively. The influence of MA on sorption of Eu(III) by γ-alumina was elucidated by batch sorption, spectroscopic techniques and surface complexation modeling, for the first time. Attenuated Total Reflection-Fourier Transform Infrared spectroscopic studies of MA sorbed on γ-alumina revealed the presence of two inner-sphere surface complexes. Batch sorption for binary (alumina-Eu(III)) and ternary (alumina-Eu(III)-MA) systems were investigated as a function of pH, Eu(III) concentration and sequential addition of Eu(III)/MA. The pH edge for Eu(III) sorption shifts to higher pH with increasing Eu(III) concentration. In ternary systems, Eu(III) sorption is significantly enhanced at pH $<$ 4.5. Eu(III) speciation on γ-alumina is independent of addition sequence of Eu(III)/MA. Time resolved fluorescence spectroscopy of Eu(III) sorbed on γ-alumina exhibited two surface species, $\equiv XOEu^{2+}$ and $(\equiv YO)_2Eu^{+}$. The enhancement in I_{616}/I_{592} and lifetime for ternary systems, as compared to binary system, at low pH, indicates the participation of Eu-MA complexes in the formation of surface species in ternary systems. The diffuse layer model has been employed to successfully model the experimental sorption profiles of binary and ternary systems, using code FITEQL 4.0, by considering the surface species identified by spectroscopic techniques.

Introduction

Nuclear energy is considered as one of the environmentally cleaner sources for production of electricity. However, reprocessing of spent nuclear fuels generates high level radioactive waste (HLW) containing long-lived actinides, fission and activation products, and thus, calls for its effective long-term management (Efremenkov, 1989; Lennemann, 1979). In order to minimize the adverse effects of these radionuclides on environment, isolation and containment of HLW in deep geological repositories (DGR) is proposed worldwide (Gens et al., 2004; Nagra, 2002). The long-lived isotopes, like ^{241}Am, ^{243}Am, ^{245}Cm or ^{246}Cm, will be present in DGR for thousands of years at depths of hundreds of meters below the surface (Hill and Harwell, 1981; Yudintsev, 2005). The decay heat of radionu-

* Corresponding author.
E-mail: aishj@barc.gov.in (A.S. Kar).

https://doi.org/10.1016/j.jes.2020.07.020
1001-0742/

clides, or natural calamities such as earth quakes, volcanic eruptions etc., could lead to release of radionuclides from the multi-barrier DGRs (Dalton, 2010), thereby increasing the risk of migration of radionuclides in the environment. The rate and duration of heat released due to radioactive decay can affect the integrity of the waste form and enhance corrosion of canisters in the proposed DGR systems. Actinides can also enter the biosphere through other routes, such as accidental release from nuclear facilities, migration in the geosphere from underground nuclear test sites, etc. The release of radionuclides into the biosphere may lead to their interaction with different components of the aquatic environment namely, complexing anions, colloids, sediments, which in turn may alter the migration of radionuclides.

Sorption of actinides onto colloids/mineral oxides is one of the important processes that governs the migration of actinides in aquatic environment. Further, sorption is known to be influenced by the presence of inorganic and organic complexing anions in the water bodies (Kersting et al., 1999; Metz et al., 2012; Mccarthy et al., 1998). This necessitates to study the migration of radionuclides in the environment by identifying the potential interaction mechanisms between the radionuclides and mineral oxides/clays in presence of complexing anions which includes both low and high molecular weight carboxylic, amino, fulvic, humic acids etc. Low molecular weight organic acids are widely distributed in ground and surface water as well as in soil in the concentration range of ng/L to μg/L. They are mainly derived from biogenesis processes such as root exudates, microbial secretions, and decomposition of plants and animals (Prapaipong et al., 1999; Thurman, 1985). For instance citric, oxalic and malonic acids are mainly released into the environment through root exudates (Strobel, 2001; Tuason, 2009). The influence of complexing anions on sorption of lanthanides/actinides by mineral oxides has been extensively studied (Fairhurst et al., 1995; Kornilovich et al., 2000; Tan et al., 2009; Wenming et al., 2001).

The effect of low molecular weight organic complexing anions on the sorption of trivalent lanthanides/actinides by various mineral oxides has been investigated in the past (Darioetal., 2006; Kasar et al., 2015; Tits et al., 2005). The increase in iso-saccharinic acid and gluconic acid concentration (10^{-4} -10^{-7}mol/L) resulted in decreased sorption of Eu(III)/Am(III) onto calcite at pH 13.3 (Tits et al., 2005). Similarly, a decrease in Eu(III) sorption was observed on TiO_2 and cement at pH 12.5 with increasing concentration of EDTA, DTPA, NTA, citric, oxalic, gluconic and iso-saccharinic acid (Dario et al., 2006). The pH dependent sorption studies of Eu(III) on anatase in presence of citric acid exhibited slight enhancement in Eu(III) sorption at lower pH, whereas sorption was reduced in the intermediate pH range (5-8) (Kasar et al., 2015).

Aluminium has an abundance of ~8% in the earth crust. Though the natural abundance of pure aluminum oxides and hydroxides is low, the major contributors of aluminum in the earth crust are aluminosilicate minerals. In addition, aluminosilicate minerals, such as bentonite, are proposed buffer/backfill material for DGR. Aluminosilicate minerals possess aluminol sites and therefore, the studies on binding of aluminol sites with radionuclides would provide insights into the mechanism of radionuclide sorption on aluminosilicate minerals.

Characterization of Eu(III) surface species on alumina using different spectroscopic techniques along with the surface complexation modeling of Eu(III) sorption profile, are well documented (Kumar et al., 2013; Rabung et al., 2000). Only few studies have been reported on the effect of low molecular weight organic acids on Eu(III) sorption by alumina (Alliot et al., 2006; Alliot et al., 2005; Moreau et al., 2016). These studies explain the uptake of Eu(III)/Am(III) sorption on alumina in presence of complexing anions (acetic, oxalic and carbonic acids) based on the suggested formation of synergic surface complexes. Moreover, at very high ligand to Am(III)/Eu(III) ratios (for oxalate $\geq 10^5$ and carbonate $\geq 5\times10^5$mol/L), a suppression in the Eu(III)/Am(III) sorption was reported due to formation of aqueous Eu(III)/Am(III)-ligand complexes (Alliot et al., 2006, 2005). Depending upon the type of substituents, their position and number, aromatic acids are known to affect Eu(III) sorption to different extents on mineral oxides. 4-hydroxybenzoic acid was not found to have any effect on sorption of Eu(III) by alumina, while 3,4-dihydroxybenzoic acid enhanced Eu(III) sorption by alumina. Time resolved fluorescence spectroscopy(TRFS) studies showed the formation of a ternary surface complex with the former acid. However, the surface complex characteristics in case of the latter acid were found close to the Eu(III)-3,4-dihydroxybenzoic acid complex (Moreau et al., 2016). The study by Moreau et al. (2016) is the only published report wherein batch sorption, spectroscopy and modeling have been used to understand effect of aromatic organic acid on the Eu(III) sorption by α/γ-alumina.

The present study is the first comprehensive report on the role of malonic acid (MA), a naturally occurring aliphatic organic acid, in modifying the Eu(III) speciation on γ-alumina. The effect of MA on sorption of Eu(III) by γ-alumina is studied by generating experimental sorption data. The surface complexes of binary (alumina-MA; alumina-Eu(III)) and ternary (alumina-Eu(III)-MA) systems were characterized by using Attenuated total reflection-Fourier transform infrared (ATR-FTIR) spectroscopy and TRFS, respectively, which served as a guide for the surface complexation modeling (SCM) of both the systems.

1. Materials and methods

1.1. *Chemicals and materials*

All the chemicals used in the experiments were of analytical reagent (AR) grade unless specified. NaCl (SD Fine Chemicals, Mumbai, India) was used for maintaining ionic strength. MA (Sigma-Aldrich, St. Louis, MO, USA) was used as received. The Eu(III) stock solution was prepared by dissolving appropriate amount of Eu_2O_3 (Merck, Darmstadt, Germany, spectroscopic grade) in concentrated HNO_3 and diluting it with 0.1 mol/L HNO_3. The working solution of Eu(III) was prepared by evaporating the required volume of Eu(III) stock solution to dryness and made up to the required volume using 0.1 mol/L HCl. Detailed preparation and standardization methodology of Eu(III) stock solution has been described elsewhere (Patel et al., 2019).

$CaCl_2$ (Merck) and $AlCl_3$ (Merck) were used for the preparation of calcium malonate and aluminum malonate aqueous solutions. All solutions and suspensions were prepared with Millipore water (18 MΩ·cm). $^{152+154}$Eu was used as a radiotracer for Eu(III) sorption studies. γ-alumina (Degussa, Aluminium Oxide C, Evonik Corporation USA) was used in this work. Prior to its use, γ-alumina was purified by following a reported procedure (Kumar et al., 2013; Rabung et al., 2000). The powder was vacuum dried at 50°C and used for characterization and further experiments. A commercial ion chromatograph (IC) (DX 500 model, Sunnyvale, CA 94085, USA) consisting of a gradient pump and suppressed conductivity detector was employed for quantifying malonic acid. The pH of all the suspensions were measured on a pH meter (Lab-India Analytical instruments PVL, West Bengal, India) and pH was adjusted by addition of dilute HCl/NaOH.

1.2. *Characterization of γ-alumina*

The X-ray diffraction (XRD) pattern of purified γ-alumina was recorded, at ambient temperature on a Rigaku Miniflex 600 X-ray diffractometer (Rigaku Miniflex 600, USA) using Ni filtered Cu Kα X-rays ($\lambda = 1.5418$ Å). The data were collected at room temperature over 2θ in the range of 5 to 80° with a scan rate of 2°/min.

1.3. *Batch sorption experiments*

1.3.1. *γ-alumina-MA and γ-alumina-Eu(III) binary systems*

All sorption experiments were performed at 25(±1)°C under controlled N_2 atmosphere. For this purpose, suspensions were prepared in boiled water and by purging continuously with nitrogen before and after the addition of MA/Eu(III). γ-alumina suspensions were prepared in 40 mL polypropylene tubes by suspending washed alumina powder in 0.1 mol/L NaCl solution to attain a solid to liquid ratio (S/L) of 5 g/L. The suspensions were left for 24 h to achieve the equilibration of γ-alumina surface sites with Na^+, before addition of Eu(III)/MA.

A set of experiments for γ-alumina-MA binary system (as Al-MA_{sorb}) were carried out by keeping MA concentration as 8×10^{-4} mol/L whereas for the γ-alumina-Eu(III) system (as Al-Eu(III)), $^{152+154}$Eu radiotracer solution with 1.72×10^{-6} mol/L Eu(III) was added to the equilibrated γ-alumina suspensions. For determining the equilibration time for the sorption of MA in Al-MA_{sorb} and Eu(III) in Al-Eu(III) systems, kinetic studies were carried out at pH 5.5. To obtain the kinetic profile of the systems, the suspensions were removed from equilibration at suitable time intervals. The suspensions were centrifuged at 16,000 r/min for 1 hr followed by MA estimation by ion chromatography (DIONEX DX-500) and radiometric assay of $^{152+154}$Eu in the supernatants.

The IC separation of MA was realized on an anion exchange column (Ion Pac AS11 HC) along with its guard column and by using a mobile phase of 7 mmol/L NaOH solution. For the determination of MA, a conductivity detector (ED 50A) coupled with an anion self-regenerated suppressor (ASRS II) was employed. The suppressor is used between the analytical column and the detector to reduce the eluent conductivity significantly. This enhances the detector response. The limit of detection (LOD) of MA was found to be 9.6×10^{-5} mol/L.

Percentage sorption of MA by γ-alumina was determined by comparing MA concentration determined in the supernatant solutions and with the control solution, which was prepared in the same manner but without sorbent.

In case of the Al-Eu(III) binary system, the concentrations of Eu(III) in the supernatant and control solutions were estimated radiometrically using a NaI(Tl) detector coupled to a 4096 channel analyser gamma spectrometer. For further sorption experiments, based on the results of kinetic studies, the equilibration time was fixed. Batch sorption experiments of Al-MA_{sorb} and Al-Eu(III) systems were carried out in pH range 2-7 with 8×10^{-4} mol/L of MA whereas the sorption of Eu(III) was studied at two different concentrations; 1.72×10^{-8} mol/L and 5×10^{-5} mol/L.

Percentage sorption of Eu(III) by γ-alumina was quantified using the following Equation.

$$\text{Sorption} = \frac{A_0 - A}{A_0} \times 100\% \quad (1)$$

where, A_0 and A are the initial and final activities of $^{152+154}$Eu, respectively.

The dissolution of γ-alumina was estimated both in the absence and presence of MA for pH 2-7 range. The concentration of aluminum in the supernatant of the suspensions, after equilibration, was determined by ICP-OES (Spectro Arcos High Resolution ICP-OES spectrometer, Germany).

1.3.2. *γ-Alumina/Eu(III)/MA ternary systems*

In order to determine a suitable equilibration time for sorption, kinetic studies were carried out at pH 5 for the sorption of Eu(III) in presence of MA. Observations were also made to know if any changes in the kinetics of sorption occurred when the sequence of adding the reagents, MA (8×10^{-4} mol/L) and Eu(III) (1.72×10^{-8} mol/L), were changed. In addition, the effect of different addition sequences of MA and Eu(III) on Eu(III) sorption by γ-alumina was also studied as a function of pH (2-7). There are two addition sequences denoted as (Al-Eu(III)-MA) and (Al-MA-Eu(III)). The procedure followed in the first sequence, (Al-Eu(III)-MA) is Eu(III) was pre-equilibrated initially with γ-alumina suspensions for 24 h(s) prior to the addition of MA whereas for the second sequence, (Al-MA-Eu(III), the MA was pre-equilibrated with γ-alumina for 24 h(s) prior to the addition of Eu(III). The subsequent steps used for the quantification of Eu(III) sorption by γ-alumina were the same as described for binary systems in Section 1.3.1.

1.4. *ATR-FTIR spectroscopy*

IR spectra of aqueous, as well as sorbed MA, were recorded with a FTIR spectrometer (Bruker, Ettlingen 76275, Germany) equipped with a deuterated triglycine sulphate (DTGS) detector. The spectra were recorded using a nine-reflection ZnSe crystal. Spectra of aqueous MA in 0.1 mol/L NaCl were recorded at varying pH, using 1000 scans at a resolution of 4 cm^{-1} between 760 and 1750 cm^{-1}. To isolate malonate vibrational bands, an appropriate background electrolyte reference spectrum was subtracted from the aqueous malonate spectrum. The sample preparation methodology for IR analysis of MA sorbed on γ-alumina was similar to that used for

the sorption experiments wherein the γ-alumina suspension strength (S/L) and MA concentration were maintained as 5 g/L and 8×10^{-4} mol/L, respectively. After equilibration, Al-MA_{sorb} samples were centrifuged at 16000 r/min for 1 hr. ATR-FTIR spectra of all the MA sorbed γ-alumina samples were recorded as wet pastes spread uniformly over ZnSe crystal. Wet pastes with small quantities of supernatant were uniformly applied on the surface of the crystal to record the spectrum. Owing to the inherent presence of carbonate as an impurity in γ-alumina, the IR spectrum of γ-alumina is dominated by strong symmetric and asymmetric vibration peaks of $-COO^{\cdot}$. Therefore, the spectrum of γ-alumina without any ligand was subtracted from the sorbed MA spectrum where the pH was maintained same in both cases to obtain vibrational signatures of sorbed malonate on γ-alumina.

To get an insight into the type of surface complex (inner or outer sphere) formed by malonate on γ-alumina, the aqueous Al-malonate (pH 3.5), Eu(III)-malonate (pH 5.5) and Ca(II)-malonate (pH 6) complexes were prepared with metal to ligand ratios of 3:2, 3:2 and 1:1, respectively. The ATR-FTIR spectra of these aqueous complexes were recorded in a similar manner as described above (1000 scans at a resolution of 4 cm^{-1} between 760 and 1750 cm^{-1}). Data collection and spectral analysis, including background subtraction, were performed using instrument software (OPUS software). The spectra were converted into DPT files and analyzed in origin 6.0.

1.5. TRFS measurements

TRFS measurements were carried out using Edinburgh nF-900 instrument (Edinburgh Kirkton Campus, EH547DQ, UK) with a Xe lamp as an excitation source, M-300 as excitation and emission monochromators and a Peltier cooled photo multiplier tube as detector. The excitation wavelength was fixed at 238 nm, while the time range for fluorescence decay data was set at 4 ms. The emission spectra were acquired in the wavelength range of 565-650 nm. For the TRFS measurements, sample preparation was similar to that adopted for the sorption studies. The concentrations of Eu(III) and MA were 5×10^{-5} and 8×10^{-4} mol/L, respectively.

With a view to investigate the effect of addition order of metal ion and ligand to the γ-alumina suspension, using TRFS, two sets of samples pertaining to Al-Eu(III)-MA) and Al-MA-Eu(III)) systems were prepared.

TRFS measurements were also carried out in aqueous solutions containing Eu(III) and MA, with a metal to ligand ratio of 1:16 (as in the sorption experiments) and Eu(III)of 5×10^{-4} mol/L and MA of 8×10^{-3} mol/L.

1.6. Speciation calculations

Aqueous speciation of Eu(III) as a function of pH was obtained by the geochemical equilibrium speciation code VISUAL MINTEQ 3.1. The stability constants of Eu-MA complexes were available in the database of the speciation codes, while those for Eu(III) complexes with OH^- and MA were incorporated at zero ionic strength in the database from literature (Bradbury and Baeyens, 2002; Martell and Smith, 2003). The log*K* values of different complexes at infinite dilution and 25°C, considered in the calculations, are given in (**Appendix A Table S1**). Since the experiments were performed in N_2 controlled atmosphere, carbonate contribution was not considered in aqueous speciation.

Table 1 – Summary of site type, site capacity, protolysis constant of γ-alumina surface (Kumar, et al., 2013) and complexation reactions and constants for Eu(III)/MA sorption on γ-alumina.

Surface characteristics	Value
Specific surface area	203 m^2/g
Suspension Strength	5 g/L
Site density	0.4 sites/nm^2
Surface sites	6.8×10^{-4} mol/L
Protolysis reaction	$\log K_{protolysis}$
$\equiv AlOH + H^+ \leftrightarrow \equiv AlOH_2^+$	7.2 ±0.2
$\equiv AlOH - H^+ \leftrightarrow \equiv AlO^-$	-9.1 ±0.1
Surface complexation reaction of Eu(III)	log*K*
$\equiv SOH + 2H^+ + MA^{2-} \leftrightarrow \equiv SMAH^0 + H_2O$	14.8 ± 0.1
$\equiv SOH + H^+ + MA^{2-} \leftrightarrow \equiv SMA^- + H_2O$	9.1 ± 0.4
$\equiv XOH + Eu^{3+} \leftrightarrow \equiv XOEu^{2+} + H^+$	2.7 ± 0.3
$\equiv (YOH)_2 + Eu^{3+} \leftrightarrow (\equiv YO)_2Eu^+ + 2H^+$	-0.7 ± 0.1
$\equiv XOH + MA^{2-} + Eu^{3+} + H^+ \leftrightarrow \equiv XMAEu^{2+} + H_2O$	16.5 ± 0.5
$XOH + MA^{2-} + Eu^{3+} \leftrightarrow \equiv XOEuMA^0 + H^+$	9.7 ± 0.2
$\equiv 2YOH + MA^{2-} + Eu^{3+} \leftrightarrow \equiv (YO)_2EuMA^- + 2H^+$	5.4 ± 0.4

1.7. Modeling of sorption data

The sorption profile for the Al-MA_{sorb}, Al-Eu(III), Al-Eu(III)-MA and Al-MA-Eu(III) systems were fitted using the code FITEQL 4.0 (Herbelin and Westall,1999), by considering the diffuse layer model. The model defines the oxide-water interface as two parallel layers of charge, namely, surface charge layer and a diffuse layer of counter ions in solution. The Gouy-Chapman distribution of ions was assumed for the diffuse layer (Dzombak and Morel, 1990). The site types, capacity and protolysis constants of γ-alumina (Table 1), given by Kumar et al. (2013), have been used in the present study.

2. Results and discussion

2.1. Characterization of purified γ-alumina

Appendix A Fig. S1 shows the XRD pattern of purified γ-alumina. The peaks at 19.02, 46.28 and 68.02° are in close agreement with the CPDS database reference no. 00-010-0425 for γ-alumina (Rozita et al., 2010). Since γ-alumina suspensions are known to be thermodynamically unstable in aqueous solutions and undergo transformation to a more stable phases like bayerite, boehmite, or gibbsite depending on reaction time (Lefevre et al., 2002), XRD of γ-alumina after purification process confirms the stability of γ-alumina. The specific surface area (203 m^2/g) and the pH_{PZC} (8.5) of γ-alumina were reported in one of our earlier studies (Kumar et al., 2013).

2.2. Kinetic study

Fig. 1a shows the sorption of Al-MA_{sorb}, Al-Eu(III), Al-Eu(III)-MA and Al-MA-Eu(III) systems as a function of contact time

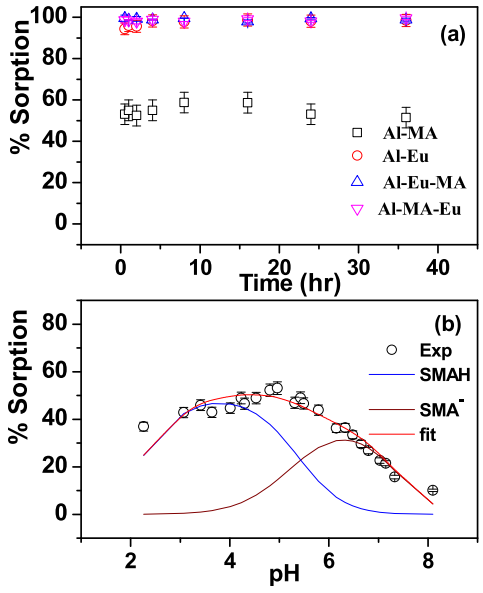

Fig. 1 – (a) Kinetics study of binary (Al-MA and Al-Eu(III)) and ternary(Al-MA-Eu(III) and (Al -Eu(III)-MA) systems. (b) MA sorption on γ- alumina as a function of pH; Solid line corresponds to the modeled data using the thermodynamic sorption model. MA = 8 x 10^{-4} mol/L, Eu(III) = 1.72 x 10^{-8} mol/L, S/L = 5 g/L, I = 0.1 mol/L NaCl.

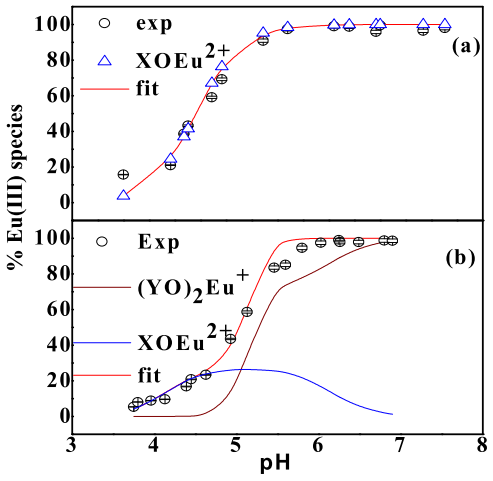

Fig. 2 – Eu(III) sorption on γ-alumina as a function of pH. (a) Eu(III) = 1.72 x 10^{-8}mol/L, (b) Eu(III) = 5 x 10^{-5}mol/L; S/L = 5 g/L, I = 0.1 mol/L NaCl.

at pH 5.5. The sorption equilibrium reached rapidly within 0.5 hr for all the systems. For further sorption studies, the contact time was fixed as 24 hr, to ensure equilibrium sorption in all the systems. Sorption kinetics of metal ions on variety of sorbents have been evaluated by employing different kinetic models like pseudo first order model, pseudo second order model, Elovich model (Ho and Mckay, 1998). Among all the kinetic models, pseudo second order kinetic model describes sorption kinetics better for low initial concentration of sorbates. The linearized form of pseudo second-order rate equation is expressed as (Ho and Mckay, 1998):

$$\frac{t}{q_t} = \frac{1}{k_2 q_e^2} + \frac{1}{q_e} t \qquad (2)$$

where q_t (mg/g) is the amount of adsorbate adsorbed onto adsorbent at time t (hr), q_e (mg/g) is equilibrium adsorption capacity, and k_2 (g/(mg.·hr)) is the pseudo second-order rate constant of adsorption. The pseudo second order kinetic model is based on the assumption that the rate of sorption of solute is proportional to the number of active sites on the adsorbent. **Appendix A Fig. S2** shows the plot of t/q_t vs. t for all the kinetic profiles presented in Fig. 1a. The coefficient of regression for linear fitting is close to 1 (**Appendix A Table S2**) in all the cases which signifies that sorption kinetics of MA/Eu(III), in all the cases, is well described by pseudo second order kinetic model. The calculated q_e values are listed **Appendix A Table S2**. Owing to high uncertainty in k_2 values, the same has not been reported in present studies.

2.3. *Sorption of MA by γ-alumina*

MA sorption on γ-alumina as a function of pH exhibits a typical anionic sorption profile (Fig. 1b). It increases up to pH 5 and thereafter, it decreased. MA sorption is maximum at the pH numerically equal to its pKa_2 ($pKa_1 = 2.65$ and $pKa_2 = 5.27$) (Martell et al., 2001). At pH < pKa, concentration of the deprotonated MA decreases as the pH decreases which result in decreased MA sorption on γ-alumina. On the other hand, for pH > pKa, increased repulsion between the deprotonated MA and γ-alumina ($pH_{pzc} = 8.5$) results in decreased MA sorption. Thus, surface charge on γ-alumina and fraction of deprotonated MA at given pH facilitates MA interaction with γ-alumina surface via electrostatic interaction, thereby ensuring the presence of MA in vicinity of γ-alumina. Subsequently, the bond formation between MA and γ-alumina surface sites results in sorption of MA on γ-alumina.

2.4. *γ-alumina -Eu(III) binary system*

2.4.1. *Sorption of Eu(III) by γ-alumina: Effect of pH and metal ion concentration*

Fig. 2 shows Eu(III) sorption profile on γ-alumina as a function of pH, at two different Eu(III) concentrations (Eu(III) = 1.72×10^{-8} mol/L and 5×10^{-5} mol/L; S/L = 5 g/L; I = 0.1 mol/L NaCl). The sorption of Eu(III) increases slowly for pH 3-5, followed by a sharp increase in the intermediate pH range 5-7, beyond which it remains constant. **Appendix A Fig. S3a** and **Appendix A Fig. S4a** show the distribution of Eu(III) species as a function of Eu(III) concentration. For both the concentration of Eu(III), $Eu(H_2O)_9^{3+}$ predominates up to pH 7 with minor contributions from hydrolyzed Eu(III) species. Thus, the speciation calculations suggest that the sorption of Eu(III) by γ-alumina is the outcome of interaction between $Eu(H_2O)_9^{3+}$ complex and γ-alumina surface sites. In addition, the pH-edge shifts towards higher pH values with increasing Eu(III) concentration (Fig. 2a and b). Similar observations were explained by

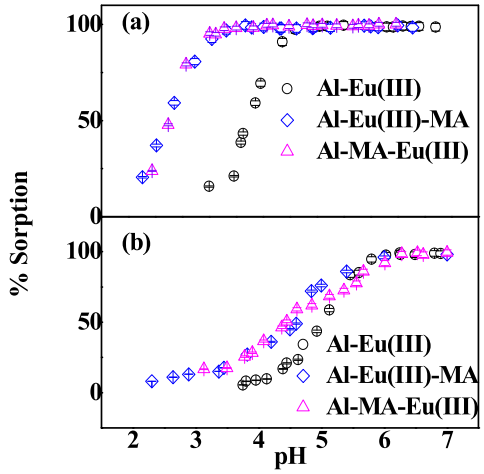

Fig. 3 – Effect of different addition sequences of Eu(III) and MA on Eu(III) sorption to γ- alumina. MA = 8 x 10^{-4}mol/L, S/L = 5 g/L, I = 0.1 mol/L, (a) Eu(III) =1.72 x 10^{-8} mol/L, (b) Eu(III) =5 x 10^{-5} mol/L.

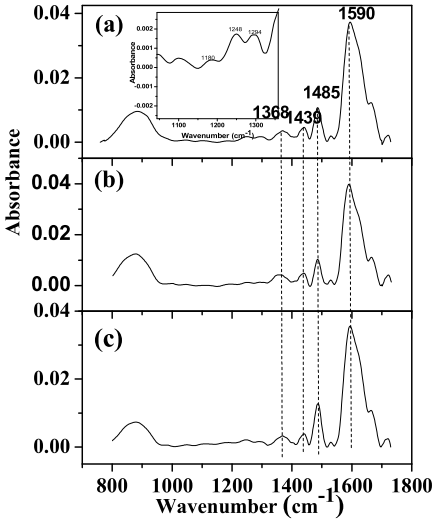

Fig. 4 – ATR-FTIR spectra of sorbed MA at different pH values (a) 2, (b) 5.5 and (c) 6.5. MA = 8 x 10^{-4} mol/L, S/L = 5 g/L, I = 0.1 mol/L NaCl.

Kumar et al. (2013) and Rabung et al. (2000) in terms of the heterogeneity of the γ-alumina surface sites.

2.4.2. *Sorption of Eu(III) by γ-alumina: Effect of MA*

Fig. 3a shows the sorption of Eu(III) (1.72×10^{-8} mol/L) by γ-alumina in presence of MA for different addition sequences (Al-Eu(III)-MA and Al-MA-Eu(III)). In the presence of MA, Eu(III) sorption is significantly enhanced for pH < 4.5. Above this pH, the sorption in ternary systems (Al-Eu(III)-MA and Al-MA-Eu(III)) behave similar to that of Al-Eu(III) system. A similar enhancement in Eu(III) sorption in the presence of MA is observed at higher metal ion concentration (5×10^{-5} mol/L), though the slope of the sorption curve is lower than that at low metal ion concentration Fig. 3b. In the presence of MA (8×10^{-4} mol/L), $Eu(H_2O)_9^{3+}$ dominates up to pH 3 with the fraction of $EuMA^+$ and $Eu(MA)_2^-$ increasing with pH for both the [Eu(III)] **(Appendix A Fig. S3b and Fig. S4b)**. Thus, the Eu(III) speciation shows that though the Eu(III) sorption profile in ternary systems appear identical to that in binary system at pH > 5, Eu(III) gets sorbed as Eu(III)-malonate surface complexes in ternary systems. The enhancement in Eu(III) sorption in the presence of MA can be rationalized in terms of the formation of strong inner-sphere surface complexes of MA on the γ-alumina surface, which facilitates Eu(III) sorption on γ-alumina at low pH values, compared to that of binary system.

The sorption data (Fig. 3a and b) in the ternary systems appear identical irrespective of the addition order of Eu(III) and MA. This essentially means that the alteration in γ-alumina surface by the introduction of Eu(III) in MA-modified γ-alumina suspension and MA in Eu(III)-modified γ-alumina suspension does not affect the sorption equilibrium in ternary system, suggesting that ternary surface complexes are more stable than binary surface complexes. This is in contrast with the observation made by Kar et al. (2014) for the sorption of Cm(III) onto silica in the presence of HIBA. In their case, when HIBA was added first the sorption was higher than the case where metal ion was added first.

2.5. *ATR-FTIR measurements*

ATR-FTIR spectra of MA sorbed on γ-alumina at different pH conditions were compared with those of aqueous MA, Ca(II)-MA, Al(III)-MA and Eu(III)-MA complexes to understand the mechanism of binding of MA onto γ-alumina.

2.5.1. *ATR-FTIR spectra of MA at different pH*

Appendix A Fig. S5 shows the spectra of MA in 0.1 mol/L NaCl at different pH. The most prominent peak at pH 2 is due to $^{\nu}C{=}O$ (1720 cm^{-1}) of protonated MA (Persson and Axe, 2005). At pH 3.2, the highly intense peak at 1581 cm^{-1} and low intensity peak at 1369 cm^{-1} are assigned to asymmetric and symmetric stretching of the COO^- group, respectively, owing to the presence of partly deprotonated MA ($pK_{a1} = 2.65$) (Persson and Axe, 2005). The complete deprotonation of MA ($pK_{a2} = 5.65$) at pH 6 causes disappearance of peak at 1720 cm^{-1} and shift in asymmetric and symmetric stretching of COO^- groups to 1564 cm^{-1} and 1354 cm^{-1}, respectively (Persson and Axe, 2005). The assignment of all vibrational bands observed in aqueous MA spectra is given in **Appendix ATable S3.**

2.5.2. *ATR-FTIR spectra of MA sorbed on γ-alumina*

ATR-FTIR spectra of MA sorbed on γ-alumina at different pH values Fig. 4 **and Appendix A Fig. S6** significantly differ from aqueous MA spectra.

A striking difference is the near absence of the vibrational frequency, $^{\nu}C{=}O$ (1720 cm^{-1}) in sorbed malonate at pH 2, which indicates that both carboxyl groups are involved in MA binding to γ-alumina surface. The shift in symmetric (1354 cm^{-1} (aqueous) to 1368 cm^{-1}) and asymmetric (1564 cm^{-1} (aqueous) to 1590 cm^{-1}) vibrational frequencies of COO^- for MA sorbed on γ-alumina indicates strong interaction of MA with γ-alumina surface (Hug and Bahnemann, 2006). Further, the comparison of ATR-FTIR spectra of MA sorbed onto γ-alumina with those of Ca-MA, Al-MA and Eu(III)-MA (**Appendix A Fig. S7**) revealed that the 1590 cm^{-1} peak in the

Table 2 – Comparison of vibrational frequencies of sorbed malonate on γ- alumina with those on other mineral oxides.

Mineral Oxide	pH range	sorb $^{\nu s}$COO	sorb $^{\nu as}$COO	$^{\delta}CH_2$ sorb	$\Delta\nu$	Ref.
Rutile/Anatase	3-9	1348/1374	1581/1582	1424/1431		Hug and Bahnemann (2006)
TiO_2	Not Specified	1352	1597	1275,1430	245	Dobson and Mcquillan (1999)
ZrO_2	Not Specified	1368	1580	1269,1433	212	Dobson and Mcquillan (1999)
Al_2O_3	Not Specified	1360	1593	1282,1445	233	Dobson and Mcquillan (1999)
Ta_2O_5	Not Specified	1381	1593	1282,1437	212	Dobson and Mcquillan (1999)
Hematite	5	1349	1631	1260,1439	282	Duckworth and Martin (2001)
γ- alumina	2-6	1368	1590	1294,1438/ 1485	222	Present study

sorbed MA exhibits a similar shift as observed for Eu(III)-MA (1584 cm^{-1}) and Al-MA (1603 cm^{-1}) complexes. For Ca-MA (1566 cm^{-1}), which is an outer-sphere complex, vibrational frequencies of COO^- is close to that of un-complexed MA (1564 cm^{-1}). Thus, the shift in symmetric and asymmetric vibrational frequencies of COO^- and comparison with Al-MA and Eu(III)-MA aquo complexes indicate the formation of inner-sphere complexes between MA and surface sites on γ-alumina. The bands at 1438 cm^{-1}(m) and 1487 cm^{-1}(s) in the entire pH range, which are attributed to -CH_2 bending, are significantly enhanced as compared to aqueous malonate. It is regarded as the signature of a strained surface structure, suggesting that MA co-ordination on γ-alumina occurs via chelation to a single surface metal ion (Dobson and Mcquillan 1999; Lenhart, et al., 2001). In addition, two weak peaks at 1180 cm^{-1} and 1248 cm^{-1} were due to $^{\nu}$C-OH and $^{\delta}$CCH, respectively.

2.5.3. *Correlation of $\Delta\nu_{as\text{-}s}$ with the structure of sorbed MA complex*

Hug and Bahnemann (2006) postulated that the metal possesses monodentate carboxylate binding when $\Delta\nu_{as\text{-}s\ (aqueous)} < \Delta\nu_{as\text{-}s\ (complex)}$, whereas $\Delta\nu_{as\text{-}s\ (aqueous)} > \Delta\nu_{as\text{-}s\ (complex)}$ indicates bidentate carboxylate binding. However, not all bidentate chelating or bridging coordinated complexes follow the trend, $\Delta\nu_{as\text{-}s\ (aqueous)} > \Delta\nu_{as\text{-}s(complex)}$ (Hug and Bahnemann, 2006). Such deviations may be observed, as the above correlations were derived from moieties having one carboxylate group. In the present study, $\Delta\nu_{as\text{-}s}$ has been found to be ~222 cm^{-1} for sorbed malonate spectra, which is higher than that of aqueous malonate (212 cm^{-1}). Though this indicates towards monodentate binding of MA on γ-alumina, the absence of the vibrational frequency for $^{\nu}$C=O (1720 cm^{-1}) rules out such monodentate MA coordination.

The FT-IR studies of metal malonate complexes, having bidentate mononuclear structure as revealed from EXAFS investigations, also showed higher $\Delta\nu_{as\text{-}s}$ value compared to the aqueous malonate (Clausén et al., 2003). The higher $\Delta\nu_{as\text{-}s}$ value of sorbed species for a bidentate mononuclear complex was attributed to the reduced symmetry of the carboxyl group of the ligand binding with a surface metal atom, resulting in a broadening in the carbon-oxygen oscillator (Duckworth and Martin, 2001). This, coupled with the near absence of the 1720 cm^{-1} peak in the ATR-FTIR spectra of MA sorbed by γ-alumina, indicates the formation of bidentate mononuclear surface complexes.

The structural investigation of sorbed MA on various mineral oxides also exhibited a similar type of MA binding on to the mineral oxide surfaces (Table 2). Thus, IR spectral analysis reveals that MA is sorbed on γ-alumina as a bidentate mononuclear species(**Appendix A Fig. S8a**). However, the weak vibrational peaks due to $^{\nu}$C-OH and $^{\delta}$CCH and enhancement of bands at 1438 cm^{-1}(m) and 1487 cm^{-1}(s) indicate the formation of an additional surface complex, a protonated bidentate species **(Appendix A Fig. 8b).**

2.6. *TRFS study*

Eu(III) displays strong luminescence spectra corresponding to de-excitation of $^5D_0$ level to ^7F_i level (I = 0 to 4). The emission at 592 nm is due to magnetic dipole transition and hence less sensitive to change in the chemical environment around the metal ion, while that at 616 nm (electric dipole transition) is termed "hypersensitive" and sensitive to change in chemical environment around the metal ion. The ratio of the luminescence intensity at 616 and 592 nm (called asymmetry ratio) provides information about europium speciation. The lifetime of $^5D_0$ state of Eu(III) increases with the substitution of the coordinated water molecules by the complexing ligand. The number of water molecules in the primary coordination sphere of Eu(III) was calculated from the lifetime (τ, ms), using the empirical formula proposed by Kimura et al. (2001), as given below.

$$n(H_2O) \pm 0.5 = \frac{1.07}{\tau} - 0.62 \quad (3)$$

2.6.1. *TRFS of Eu(III) - MA_{aqs} complexes*

Fluorescence emission spectra of Eu(III) (5×10^{-4} mol/L) complexes with MA (8×10^{-3} mol/L) in 0.1 mol/L NaCl at pH 3, 4 and 6 are shown in **Appendix A Fig. S9.** It is observed that the asymmetry ratio I_{616}/I_{592} increases from 1.64 to 2.93 with increase in pH. The lifetime data is well fitted by considering mono-exponential decay with its value changing from 142 to 192 μs as pH is increased from 3 to 6. This corresponds to a decrease in the number of water molecules present in the first co-ordination shell from 8-7 (for 142 μs) to 6-5 (for 192 μs). The data indicates the formation of inner-sphere Eu(III) complexes with MA, with the species as ML and ML_2. Similar speciation of Eu-MA complexes has been reported by using potentiometry and fluorescence spectroscopy (Wang et al., 2000).

2.6.2. *TRFS of Eu(III) sorbed onto γ-alumina*

Fluorescence emission spectra of Eu(III) (5×10^{-5} mol/L) sorbed on γ-alumina (5 g/L) at pH 4 and 6.5 are shown in Fig. 5a.

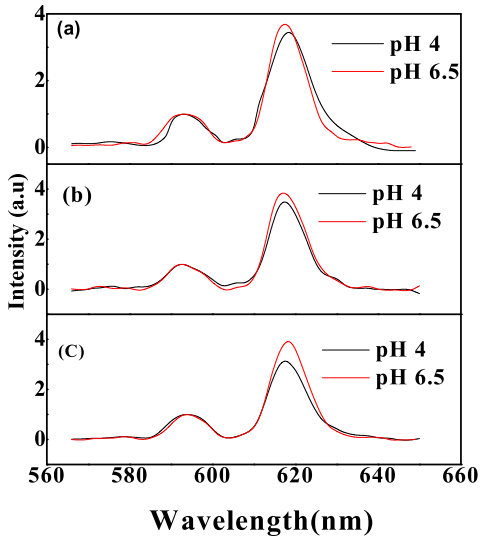

Fig. 5 – Time resolved fluorescence emission spectra of sorbed Eu(III) on γ-alumina; (a) Al-Eu(III), (b) Al-Eu(III)-MA, (c) Al-MA-Eu(III). Eu(III) = 5 x 10^{-5}mol/L, MA = 8 x 10^{-4}mol/L; S/L = 5 g/L, I = 0.1 mol/L NaCl.

The increase in the asymmetry ratio (I_{616}/I_{592}) indicates the formation of a more asymmetric surface complex at higher pH.

Appendix A Fig. S10a shows a typical fluorescence decay curve for Eu(III) sorbed on γ-alumina at pH 6.5, which was fitted into multi-exponential functions from 50 µs to 4 ms, so as to obtain the fluorescence lifetime of species. The best fit was obtained with two lifetime components namely 1 and 2. The asymmetry ratio for the components 1 and 2 changed from 2.2 to 2.4 and 2.9 to 3.1, respectively (Table 3 and **Appendix A Fig. S11a and S11b).** The lifetime values corresponding to the two components (τ_1 andτ_2) as a function of pH are also listed in Table 3. The lower lifetime value (τ_1) increases from 166 to 185 μs, while the higher lifetime value (τ_2) changes from 448 to 464 μs with increase in pH. The number of H_2O molecules in the first co-ordination shell, calculated using Eq. (3), indicates that the surface complex corresponding to τ_1 has 5-7 water molecules around Eu(III). On the other hand, the component τ_2 corresponding to 1-2 water molecules indicates that Eu(III) is sorbed as a multi-dentate surface species, which is in agreement with the previously reported EXAFS and TRLFS investigations (Kumar et al., 2013; Rabung et al., 2000).

2.6.3. *TRFS of Eu(III) sorbed on γ-alumina in presence of MA*

The fluorescence emission spectra and representative fluorescence decay curves for the different orders of addition are presented in Fig. 5b and c, and **Appendix A Fig. S10b** and **S10c,** respectively. The asymmetry ratio with the respective lifetime values (Table 3 and **Appendix A Fig. S11c-f**) remain nearly constant at all pH values, confirming formation of similar Eu(III) surface complexes for both the addition sequences.

The asymmetric ratio and the lifetime of component 1 in the ternary Al-Eu(III)-MA and Al-MA-Eu(III) systems (185 μs) are higher than that in the binary Al-Eu(III) system (166 μs) at low pH (~ 4), whereas the lifetime of component 2 is the same

Table 3 – Spectroscopic characteristics of Eu(III)-MA (binary), Al-Eu(III) (binary) and Al- Eu(III)-MA, Al-MA-Eu(III) (ternary) systems as a function of pH

1.Eu(III)-$MA_{(aqs)}$					
pH	3		4		6
Component	τ_1		τ_1		τ_1
Lifetime (µs)	142		162		192
$^5D_0\rightarrow{}^7F_2/^5D_0\rightarrow{}^7F_1$	1.6		2.04		2.34
nH_2O ±0.5	7		6		5
2. Al-Eu(III)					
pH	4.0		6.5		
Component	τ_1	τ_2	τ_1	τ_2	
Lifetime (µs)	166	448	185	464	
$^5D_0\rightarrow{}^7F_2/^5D_0\rightarrow{}^7F_1$	2.2	2.9	2.4	3.1	
nH_2O ±0.5	7	2	5	2	
3. Al-Eu(III)-MA					
pH	4.0		6.0		
Component	τ_1	τ_2	τ_1	τ_2	
Lifetime (µs)	179	429	206	442	
$^5D_0\rightarrow{}^7F_2/^5D_0\rightarrow{}^7F_1$	2.6	3.2	2.9	3.0	
nH_2O ±0.5	5	2	5	2	
4. Al-MA-Eu(III)					
pH	4		6.0		
Component	τ_1	τ_2	τ_1	τ_2	
Lifetime (µs)	185	443	191	425	
$^5D_0\rightarrow{}^7F_2/^5D_0\rightarrow{}^7F_1$	2.5	3.0	2.9	3.0	
nH_2O ±0.5	5	2	5	2	

in both the ternary and binary systems. The higher asymmetric ratio and lifetime of component 1 in the ternary system, compared to the binary system, indicate the participation of MA in the surface complexation of Eu(III) with γ-alumina surface sites. However, in case of the higher lifetime component, the denticity of the surface complex is same in the binary as well as ternary systems. This confirms that the presence of MA in Eu(III) surface complexes on γ-alumina (ternary system) does not significantly alter the binding mechanism of Eu(III) in component 2. Thus, MA containing surface species have been confirmed by TRFS in ternary systems. Likewise, there are studies wherein spectroscopic techniques have been employed to illustrate the sorption of metal ions on sorbents via organic moieties (Hu et al., 2019; Zhong et al., 2020).

2.7. *Surface complexation modeling*

Two different types of surface sites, namely, strong sites (≡XOH, high complexation strength but low in concentration) and weak sites (≡YOH, higher concentration but lower complexation strength) have been considered while modeling Eu(III) sorption by γ-alumina. The information obtained from the spectroscopy measurements and the speciation calculations of Eu(III), in the absence and presence of MA, were used as inputs in the surface complexation modeling of the sorption data.

In addition, it is important to consider the γ-alumina dissolution while modeling MA sorption (Al-MA_{sorb}) and Eu(III) sorption by γ-alumina in presence of MA (Al-MA-Eu(III) and Al-Eu(III)-MA). Fig. 6 shows the dissolution of γ-alumina in absence and presence of MA. The decrease in γ-alumina dissolution with increase in pH signifies proton promoted dissolu-

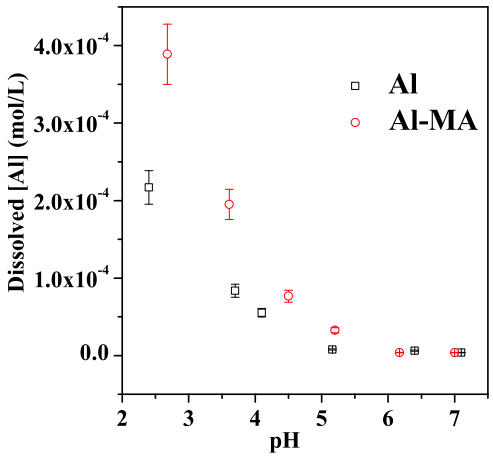

Fig. 6 – Dissolution of γ -alumina in presence and absence of MA as afunction of pH. MA = 8 x 10^{-4} mol/L, I = 0.1 mol/L NaCl, S/L = 5 g/L.

tion. In presence of MA, ligand promoted dissolution results in enhanced γ-alumina dissolution (pH < 5). The γ-alumina dissolution data was fitted into the polynomial function, as shown in **Appendix A Fig. S12**, to calculate alumina dissolution at respective pH values for the sorption systems containing MA.

2.7.1. *SCM of Al-MA$_{sorb}$ sorption data*

Since MA is in large excess compared to the strong sites, only one site (≡SOH =≡XOH + ≡YOH) was considered for modeling MA sorption byγ-alumina. The number, type and protonation state of the ligand surface complexes, obtained from the ATR-FTIR investigation, were used to constrain modeling. In addition, the stability constants of aluminum malonate aqueous complexes (**Appendix A Table 2**) were incorporated in the model (Powell and Town, 1993). The sorption of MA by γ-alumina was successfully modeled using these two surface complexes, i.e., a bidentate mononuclear complex and a protonated bidentate complex (Fig. 1b). The corresponding surface complexation reactions are represented by the following Equations.

$$\equiv SOH + 2H^+ + MA^{2-} \leftrightarrow \equiv SMAH^0 + H_2O \quad (4)$$

$$\equiv SOH + H^+ + MA^{2-} \leftrightarrow \equiv SMA^- + H_2O \quad (5)$$

The best fit log*K* values are given in Table 1. Ramos et al. (2015) modeled oxalic acid sorption on montmorillonite considering two similar inner-surface complexes, viz., >AlOxH and >AlOx$^-$.

2.7.2. *SCM of Al-Eu(III) sorption data*

Fig. 2a and b show the modeled sorption data of Eu(III) by γ-alumina as a function of pH at two different Eu(III) concentrations. In the case of low metal ion concentration, the high affinity sites dominate surface speciation. The concentration of high affinity sites has been considered as 2% of the total number of surface hydroxyl sites (Kumar et al., 2013). The fitting of the sorption data was carried out by considering only ≡XOH, as concentration of these strong sites in γ-alumina is almost two orders of magnitude higher than the concentration of Eu(III). In the case of low Eu(III) concentration, upto pH 7, $Eu(H_2O)_9^{3+}$ predominates along with minor contributions from $EuOH^{2+}$ and $EuOH_2^+$. However, no convergence was obtained when hydrolysed surface complexes were considered along with the monodentate Eu(III) surface complex (≡XOEu^{2+}). A satisfactory fit was obtained by considering only ≡XOEu^{2+} surface complexation reaction given below:

$$\equiv XOH + Eu^{3+} \leftrightarrow \equiv XOEu^{2+} + H^+ \quad (6)$$

Similar approach has been adopted in literature for modeling Eu(III)/Am(III) sorption by γ-alumina at low Eu(III) concentration (Kumar et al., 2013; Rabung et al., 2000).

The weak sites play an important role at higher concentration of Eu(III). In the present work, Eu(III) is 5×10^{-5} mol/L, and aluminol sites available for sorption are nearly 6.8×10^{-4} mol/L. Therefore, surface precipitation is ruled out as it is likely to occur only when the metal concentration is more than 1/10th of the solubility limit, and the surface coverage is more than 1/3rd of the total available surface sites (Dzombak and Morel, 1990). In the case of high Eu(III) concentration, both strong and weak sites were considered in the optimization procedure. In view of the similar speciation of Eu(III) at low and high concentrations, only non-hydrolyzed species were considered. The fluorescence decay measurements revealed the existence of two surface species containing 6-7 and 1-2 water molecules, respectively. Therefore, the optimization of the experimental data was achieved by considering monodentate (≡XOEu^{2+}) and bidentate ((≡YO)$_2$Eu$^+$) complexes. The corresponding surface complexation reactions are given in Eqs. (6) and ((7).

$$2(\equiv YOH) + Eu^{3+} \leftrightarrow (\equiv YO)_2Eu^+ + 2H^+ \quad (7)$$

The log*K* for monodentate species was found to be in agreement with that obtained for Eu(III)/Am(III) monodentate surface species on γ-alumina (Rabung et al., 2000). However, in the present study, log*K* value of −0.7 obtained for the surface complex corresponding to the "weak" site differs from the value reported (-5.0) by Kumar et al. (2013). Though Eu(III) sorption on γ-alumina was optimized using FITEQL 4.0 in both the studies, the discrepancy in log K values is the manifestation of different experimental methodologies adopted for preparing alumina suspension in both the studies.

2.7.3. *SCM of Eu(III) sorption by γ-alumina in presence of MA*

Eu(III) = 1.72 x 10^{-8}mol/L: Uptake of Eu(III) by γ-alumina in the presence of MA is independent of the order of addition, indicating similar surface speciation of Eu(III) in the both ternary systems, as confirmed by TRFS. Considering Eu(III) aqueous speciation in presence of MA **(Appendix A Fig. S3b),** the surface complex pertaining to EuMA$^+$ species on γ-alumina was considered. EXAFS and ATR-FTIR of Pb(II)-MA complex on hematite showed a metal-bridged ternary surface complex (Lenhart et al., 2001). In the present modeling exercise, consideration of ≡XOEu^{2+} and metal-bridged ≡XOEuMA^0 species did not provide any convergence between the experimental data and the fits. Similar observations were made by Moreau et al. (2016) who failed to fit the sorption data of Eu(III)

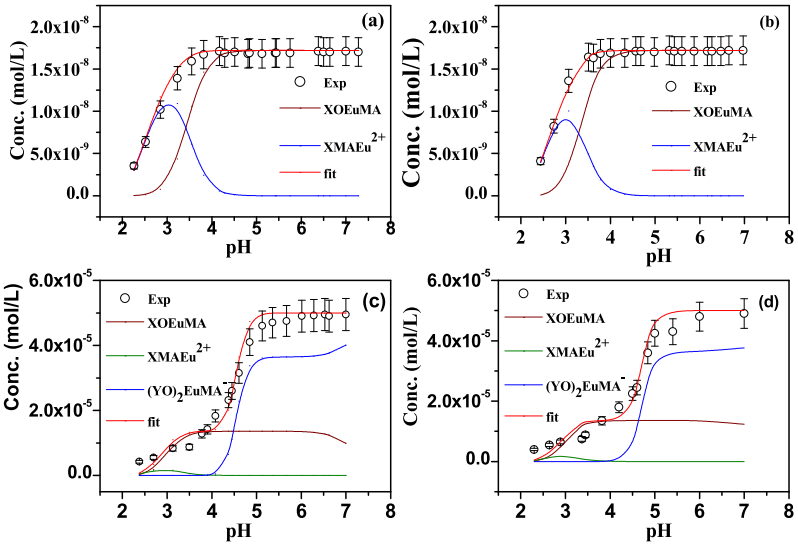

Fig. 7 – Surface complexation modeling of Eu(III) sorption by γ-alumina in presence of MA (a), (c) Al-Eu(III)-MA, (b), (d) Al-MA-Eu(III). MA = 8 x 10^{-4} mol/L, S/L = 5 g/L, I = 0.1 mol/L NaCl. Eu(III) = 1.72 x 10^{-8} mol/L (a,b), 5 x 10^{-5} mol/L (c,d).

by alumina in the presence of phenolic hydroxyl acid by considering only metal-bridged ternary surface species.

Enhancement of Eu(III) sorption by γ-alumina in presence of MA was observed in the pH range of 3-5, wherein the sorption of MA by γ-alumina was the strongest, which suggests the formation of ligand-bridged metal surface complexes. Sorption of divalent cations onto a variety of mineral oxides was successfully modeled by considering both metal-bridged and ligand-bridged ternary surface complexes (Vohra and Davis, 1997; Nowack et al., 1996). Therefore, ligand-bridged ($\equiv XOMAEu^{2+}$) and metal-bridged ($\equiv XOEuMA^{0}$) surface complexes were considered, as shown in Eqs. (8) and ((9).

$$\equiv XOH + MA^{2-} + Eu^{3+} + H^{+} \leftrightarrow \equiv XMAEu^{2+} + H_2O \quad (8)$$

$$\equiv XOH + MA^{2-} + Eu^{3+} \leftrightarrow \equiv XOEuMA^{0} + H^{+} \quad (9)$$

In the optimization of log*K* for these surface species, the log*K* of other species determined for the Al-MA_{sorb} and Al-Eu(III) binary systems were not changed. The optimized log*K* values are given in Table 1 and the fitted sorption data are shown in Fig. 7a and b.

Eu(III) = 5 x 10^{-5}mol/L: MA sorption on high affinity ($\equiv$XOH) and low affinity sites ($\equiv$YOH) has been considered to be similar. Therefore, the same sorption constants (log*K*) for MA surface species have been assumed on both the sites (Table 1).

TRFS measurements indicated the presence of two species in the ternary systems. One, involving MA containing Eu(III) surface complex (τ_1), and other species, possessing similar Eu(III) coordination environment as in the binary system (τ_2). Speciation calculations reveal that Eu(III)-MA complexes dominate the speciation at higher pH. Therefore, $(\equiv YO)_2EuMA^{-}$ (Eq. (10)) was considered for modeling the ternary systems at high Eu(III) concentration, keeping the log*K* of other species the same. Fig. 7c and d shows that metal-bridged ternary surface species dominates the surface speciation of Eu(III) at low pH, while metal-bridged bidentate ternary species dominates at higher pH. The modeling of sorption data of different addition sequence was successfully done using the same species (Fig. 7c and d).

$$2 \equiv YOH + MA^{2-} + Eu^{3+} \leftrightarrow (YO)_2EuMA^{-} + 2H^{+} \quad (10)$$

The log*K* for the surface complexes are given in Table 1.

3. Conclusions

The sorption of Eu(III) by γ-alumina was investigated in presence of MA. According batch, spectroscopic and modeling techniques, the sorption of Eu(III) by γ-alumina is strongly influenced by the presence of MA due to the surface binding of MA onto γ-alumina and the formation of Eu(III)-MA complexes.

The sorption of MA by γ-alumina followed a typical anionic profile and increased up to pH 5, above which it decreased. ATR-FTIR spectroscopy showed the signature of bidentate mononuclear and protonated bidentate MA species on γ-alumina, which were used to model MA sorption profile on γ-alumina. In addition, γ-alumina dissolution was found to be promoted by MA. Therefore, aqueous aluminum malonate complexes were considered while modeling the MA sorption.

The sorption edge for Eu(III) by γ-alumina shifted to higher pH with increase in metal ion concentration, suggesting site heterogeneity. TRFS studies revealed the existence of two surface species, based on which Eu(III) sorption data was modeled by considering monodentate ($\equiv XOEu^{2+}$) and bidentate ($\equiv YO)_2Eu^{+}$) species at high Eu(III) concentration. However, $\equiv XOEu^{2+}$ species could successfully reproduce Eu(III) sorption data at only low Eu(III)concentration.

In presence of MA, the sorption of Eu(III) by γ-alumina is enhanced in the pH range 3-5, compared to the binary Eu(III)-γ-alumina system. This has been explained in terms of ligand-bridged as well as metal-bridged surface species at low pH,

corroborated by TRFS measurements, which served as a guide for surface complexation modeling of the sorption data. The order of addition of Eu(III) and MA to the γ-alumina suspension had no effect on the sorption of Eu(III), as shown in the uptake curves and supporting TRFS studies.

The increased Eu(III) sorption in presence of MA could lead to enhanced immobilization of Eu(III) on aluminol sites, prevalent in the environment, by formation of ligand-bridged and metal-bridged Eu(III) ternary surface complexes. Thus, the present study could successfully delineate the role of MA in influencing Eu(III) sorption by γ-alumina.

Acknowledgments

Authors thank Dr. S. Jeyakumar and Dr. Sumit Kumar for fruitful discussions and suggestions. Thanks are due to Dr. Nimai Pathak for helping in fluorescence experiments. Dr. B. S. Tomar acknowledges the support from DAE towards Raja Ramanna Fellowship.

Appendix A. Supplementary data

Supplementary material associated with this article can be found, in the online version, at doi:10.1016/j.jes.2020.07.020.

REFERENCES

Alliot, C., Bion, L., Mercier, F., Vitorge, P., Toulhoat, P., 2005. Effect of aqueous acetic, oxalic and carbonic acids on the adsorption of americium onto α-alumina. Radiochim. Acta. 93 (8), 435–442.

Alliot, C., Bion, L., Mercier, F., Vitorge, P., Toulhoat, P., 2006. Effect of aqueous acetic, oxalic, and carbonic acids on the adsorption of europium(III) onto α-alumina. J. Colloid Interf. Sci. 298 (2), 573–581.

Bradbury, M., Baeyens, B., 2002. Sorption of Eu on Na- and Ca-montmorillonites: experimental investigations and modelling with cation exchange and surface complexation. Geochim. Cosmochim. Acta. 66 (13), 2325–2334.

Clausén, M., Öhman, L-O., Axe, K., Persson, P., 2003. Spectroscopic studies of aluminum and gallium complexes with oxalate and malonate in aqueous solution. J. Mol. Struct. 648 (3), 225–235.

Dalton, J., 2010. Geological Disposal Radionuclide Behaviour Status Report NDA Report no. NDA/RWMD/034, UK.

Dario, M., Molera, M., Allard, B., 2006. Sorption of europium on TiO_2 and cement at high pH in the presence of organic ligands. J. Radioanal. Nucl. Chem. 270, 495–505.

Dobson, K.D, Mcquillan, A., 1999. In situ infrared spectroscopic analysis of the adsorption of aliphatic carboxylic acids to TiO_2, ZrO_2, Al_2O_3, and Ta_2O_5 from aqueous solutions. Spectrochim. Acta. A Mol. Biomol. Spectrosc. 55, 1395–1405.

Duckworth, O.W., Martin, S.T., 2001. Surface complexation and dissolution of hematite by C_1 -C_6dicarboxylic acids at pH = 5.0. Geochim. Cosmochim. Acta 65, 4289–4301.

Dzombak, D.A., Morel, F.M., 1990. Surface Complexation Modeling: Hydrous Ferric Hydroxide. Wiley-Interscience, New York.

Efremenkov, V.M., 1989. Radioactive waste management at nuclear power plants. IAEA Bull. 4, 37–42.

Fairhurst, A.J., Warwick, P., Richardson, S., 1995. The influence of humic acid on the adsorption of europium onto inorganic colloids as a function of pH. Colloids Surf. A 99, 187–199.

Gens, R., Lalieux, P., Preter, P.D., Dierckx, A., Bel, J., Boyazis, J-P., et al., 2004. . The second safety assessment and feasibility interim report (SAFIR 2 Report) on HLW disposal in boom clay: overview of the Belgian programme. MRS Proc. 807, 1–6. doi:10.1557/proc-807-917.

Herbelin, A.L., Westall, J.C., 1999. FITEQL, A Computer Program for Determination of Chemical Equilibrium Constant from Experimental Data, Department of Chemistry, Oregon State University, Oregon, USA.

Hill, M.D., Harwell, 1981. Disposal of radioactive waste. Europhys. News 12, 9–11 http:/doi.org/10.1051/epn/19811205009.

Ho, Y.S., Mckay, G., 1998. A comparison of chemisorption kinetic models applied to pollutant removal on various sorbents. Process Saf. Environ. Prog. 76, 332–340.

Hu, B., Song, Y., Wu, S., Zhu, Y., Sheng, G., 2019. Slow released nutrient-immobilized biochar: A novel permeable reactive barrier filler for Cr(VI) removal. J. Mol. Liq. 286 (110876), 1–9. https://doi.org/10.1016/j.molliq.2019.04.153.

Hug, S.J., Bahnemann, D., 2006. Infrared spectra of oxalate, malonate and succinate adsorbed on the aqueous surface of rutile, anatase and lepidocrocite measured with in situ ATR-FTIR. J. Electron. Spectros. Relat. Phenomena. 150, 208–219.

Kar, A.S., Tomar, B.S., 2014. Cm(III) sorption by silica: effect of alpha hydroxyisobutyric acid. Radiochim. Acta 102 (9), 763–773.

Kasar, S., Kumar, S., Raut, V.V., Jeyakumar, S., Tomar, B.S., 2015. Speciation of citric acid on anatase (TiO_2)–water interface and its effect on Eu(III) sorption. Radiochim. Acta 103 (4), 305–312.

Kersting, A.B., Efurd, D.W., Finnegan, D.L., Rokop, D.J., Smith, D.K., Thompson, J.L., 1999. Migration of plutonium in ground water at the Nevada test site. Nature 397, 56–57.

Kimura, T., Kato, Y., Takeishi, H., Takahashi, Y., Minai, Y., Choppin, G.R., 2001. Determination of the hydration number of actinides and lanthanides by luminescence lifetime measurement and its application to the speciation study. In: Proceedings of the OECD/NEA Workshop on Evaluation of Speciation Technology, p. 61.

Kornilovich, B., Pshinko, G., Spasenova, L., Kovalchuk, I., 2000. Influence of humic substances on the sorption interactions between lanthanide and actinide ions and clay minerals. Adsorpt. Sci. Technol. 18 (10), 873–880.

Kumar, S., Godbole, S.V., Tomar, B.S., 2013. Speciation of Am(III)/Eu(III) sorbed on γ-alumina: effect of metal ion concentration. Radiochim. Acta 101 (2), 73–80.

Lenhart, J.J., Bargar, J.R., Davis, J.A., 2001. Spectroscopic evidence for ternary surface complexes in the lead(II)–malonic acid–hematite system. J. Colloid. Interf. Sci. 234 (2), 448–452.

Lennemann, W.L., 1979. The management of high-level radioactive wastes. IAEA Bull. 21 (4), 2–16 ISSN 0020-6067.

Lefevre, G., Duc, M., Lepeut, P., Caplain, R., Fedoroff, M., 2002. Hydration of γ-alumina in water and its effects on surface reactivity. Langmuir 18, 7330–7537.

Martell, A.E., Smith, R.M., 2003. NIST Standard Reference Database, 46.7, NIST Critically selected stability constants of metal complexes. National Institute of Standards and Technology, Gaithersburg, MD, USA.

Martell, A.E., Smith, R.M., Motekaitis, R.J., 2001. NIST Database 46. National Institute of Standards and Technology, Gaithersburg, MD, USA.

Mccarthy, J.F., Czerwinski, K.R., Sanford, W.E., Jardine, P.M., Marsh, J., 1998. Mobilization of transuranic radionuclides from disposal trenches by natural organic matter. J. Contam. Hydrol. 30, 49–77.

Metz, V., Geckeis, H., Gonzáles-Robles, E., Loida, A., Bube, C., Kienzler, B., 2012. Radionuclide behaviour in the near-field of a geological repository for spent nuclear fuel. Radiochim. Acta 100, 699–713.

Moreau, P., Colette-Maatouk, S., Gareil, P., Reiller, P.E., 2016. Influence of hydroxybenzoic acids on the adsorption of Eu(III) onto α,γ-Al_2O_3 particles in mildly acidic conditions: a macroscopic and spectroscopic study. Appl. Geochem. 74, 13–23.

Nagra, 2002. Project Opalinus Clay: Safety Report. Demonstration ofdisposal feasibility (Entsorgungsnachweis) for Spent Fuel Vitrifiedhigh-Level Waste and Long-Lived Intermediate-Level Waste NagraTechnical Report NTB 02-05, Report ISSN 1015-2636 Nagra, Wettingen, Switzerland.

Nowack, B., Lützenkirchen, J., Behra, P., Sigg, L., 1996. Modeling the adsorption of metal–EDTA complexes onto oxides. Environ. Sci. Technol. 30 (7), 2397–2405.

Patel, M.A., Kar, A.S., Kumar, S., Das, M.K., Raut, V.V., Tomar, B.S., 2019. Effect of sulfate on sorption of Eu(III) by Na-montmorillonite. Radiochim. Acta. 107 (2), 115–128.

Persson, P., Axe, K., 2005. Adsorption of oxalate and malonate at the water-goethite interface: molecular surface speciation from IR spectroscopy. Geochim. Cosmochim. Acta. 69 (3), 541–552.

Powell, H.K.J., Town, R.M., 1993. Aluminium(III)-malonate etquilibria: a potentiometric study. Aust. J.Chem 46 (5), 721–726.

Prapaipong, P., Shock, E.L., Koretsky, C.M., 1999. Metal-organic complexes in geochemical processes: temperature dependence of the standard thermodynamic properties of aqueous complexes between metal cations and dicarboxylate ligands. Geochim. Cosmochim. Acta 63 (17), 2547–2577.

Rabung, T., Stumpf, T., Geckeis, H., Klenze, R., Kim, J.I., 2000. Sorption of Am(III) and Eu(III) onto γ-alumina: experiment and modeling. Radiochim. Acta 88, 711–716.

Ramos, M.E., Emiroglu, C., García, D., Sainz-Díaz, C.I., Huertas, F.J., 2015. Modeling the adsorption of oxalate onto montmorillonite. Langmuir 31 (43), 11825–11834.

Rozita, Y., Brydson, R., Scott, A.J., 2010. An investigation of commercial gamma-Al_2O_3 nanoparticles. J. Phys. 241, 012096. doi:10.1088/1742-6596/241/1/012096.

Strobel, B.W., 2001. Influence of vegetation on low-molecular-weight carboxylic acids in soil solution-a review. Geoderma 99, 169–198.

Tan, X., Fang, M., Li, J., Lu, Y., Wang, X., 2009. Adsorption of Eu(III) onto TiO_2: effect of pH, concentration, ionic strength and soil fulvic acid. J. Hazard. Mater. 168, 458–465.

Thurman, E.M., 1985. Organic Geochemistry of Natural Waters. MartinusNijhoff/Dr. W. Junk Publishers, Boston.

Tits, J., Wieland, E., Bradbury, M., 2005. The effect of isosaccharinic acid and gluconic acid on the retention of Eu(III), Am(III) and Th(IV) by calcite. Appl. Geochem. 20 (11), 2082–2096.

Tuason, M.M., Arocena, J.M., 2009. Root organic acid exudates and properties of rhizosphere soils of white spruce (Piceaglauca) and subalpine fir (Abieslasiocarpa). Can. J. Soil. Sci. 89 (3), 287–300.

Vohra, M.S., Davis, A.P., 1997. Adsorption of Pb(II), NTA, and Pb(II)–NTA onto TiO_2. J. Colloid Interf. Sci. 194 (1), 59–67.

Wang, Z-M., Burgt, L.V.D., Choppin, G., 2000. Spectroscopic study of lanthanide(III) complexes with aliphatic dicarboxylic acids. Inorganica Chimica Acta 310 (2), 248–256.

Wenming, D., Xiangke, W., Xiaoyan, B., Aixia, W., Jingzhou, D., Zuyi, T., 2001. Comparative study on sorption/desorption of radioeuropium on alumina, bentonite and red earth: effects of pH, ionic strength, fulvic acid and iron oxides in red earth. Appl. Radiat. Isot. 54 (4), 603–610.

Yudintsev, S.V., 2005. An international spent nuclear fuel storage facility: exploring a russian site as a prototype. In: Proceedings of an International Workshop Chapter: Immobilization of High Level Waste: Analysis of Appropriate Synthetic Waste Forms209-290, pp. 208–224.

Zhong, X., Liang, W., Lu, Z., Hu, B., 2020. Highly efficient enrichment mechanism of U(VI) and Eu(III) by covalent organic frameworks with intramolecular hydrogen-bonding from solutions. Appl. Surf. Sci. 504, 144403. https://doi.org/10.1016/j.apsusc.2019.144403.